Original article

Development of the evaluation system for barrier functions of engineered epithelial lumens

CrossMark

Kazuya Furusawa[*], Takeomi Mizutani, Naoki Sasaki

Faculty of Advanced Life Science, Hokkaido University, Kita-ku, Kita 10 Nishi 8, Sapporo, Hokkaido, Japan

ABSTRACT

We have investigated the effects of a diameter of engineered epithelial lumen on cellar architectures and a barrier function. For this investigation, we have developed a system to evaluate the barrier function of engineered epithelial lumens. To test the utility of our system, we constructed the engineered epithelial lumens by culturing Madin−Darby Canine Kidney cells (MDCK) on the gold wires with different diameters ranging from 50 μm−200 μm. Confocal laser scanning microscopy revealed that long actin stress fibers and a low focal adhesion density were observed at the gold wire diameter of 200 μm, whereas the mesh-like morphology consisted of short actin stress fibers and high focal adhesion densities were found at the gold wire diameters of 50 μm and 100 μm. The expression pattern of ZO-1 that localizes at the tight junction was independent on the gold wire diameter. The electrical impedance measurement indicates that the barrier function for the samples constructed at the gold wire diameter of 200 μm was significantly higher than those at the gold wire diameters of 50 μm and 100 μm. The difference in the barrier functions of epithelial lumens might be attributed to the changes in cellular architectures with increasing the curvature of gold wire.

Introduction

Epithelial lumens, such as blood vessel, lymphatic vessel, and kidney tubule, play the roles of transport ducts for oxygen, nutrients, cells, and waste products. An inner surface of the epithelial lumen is covered by an epithelial cell sheet. The epithelial cell sheet prevents leakage of fluid flowing in the epithelial lumens. In addition, the epithelial cell sheets are interfaces for exchanging oxygen, ions, nutrients, and waste products. The selective exchanges are regulated by the tight junction [1,2].

Introducing the epithelial lumens into engineered tissues is a prerequisite for constructing functional and healthy engineered tissues. Therefore, many methods for introducing the epithelial lumens into the engineered tissues have been developed in the tissue engineering and the regenerative medicine fields [3–6]. However, the engineered epithelial lumens without appropriate barrier functions cannot be used as transport ducts. Therefore, we must evaluate the barrier functions for the epithelial lumens introduced in the engineered tissues.

The fluid leakage can be detected by perfusing media with fluorescent dye-conjugated macromolecules, such as dextran and polystyrene latex beads, into the epithelial lumens [3,7,8]. By contrast, the barrier functions for the epithelial cell sheet have been characterized by the transepithelial resistance (TER) [9–11]. TER can be determined by analyzing the electrical impedance spectrum. However, almost systems to measure the electrical impedance spectrum have been designed for two-dimensional epithelial cell sheet. There have been only a few systems to characterize TER for epithelial lumens [11], but they were designed for epithelial lumens with large diameters and applications were also limited.

Therefore, in this study, we have developed a system for evaluating the barrier functions of the epithelial lumens. The system consists of cylindrical and central rod electrodes. The epithelial lumens can be directly constructed on the surface of the cylindrical and/or central rod-like electrodes. By selecting the diameter of the central rod-like electrode, we can investigate an effect of the diameter for the epithelial lumen on the barrier functions. Recently, it was reported that the diameter of epithelial lumens affects cellular architectures, such as an orientation of actin filaments and a focal adhesion density [12]. The diameter dependences on cellular architecture could influence the barrier functions of epithelial lumens. Therefore, we have investigated effects of diameter of

---

* Corresponding author. Fax: +81 11 706 4493.
  E-mail address: kfurusawa@sci.hokudai.ac.jp (K. Furusawa).
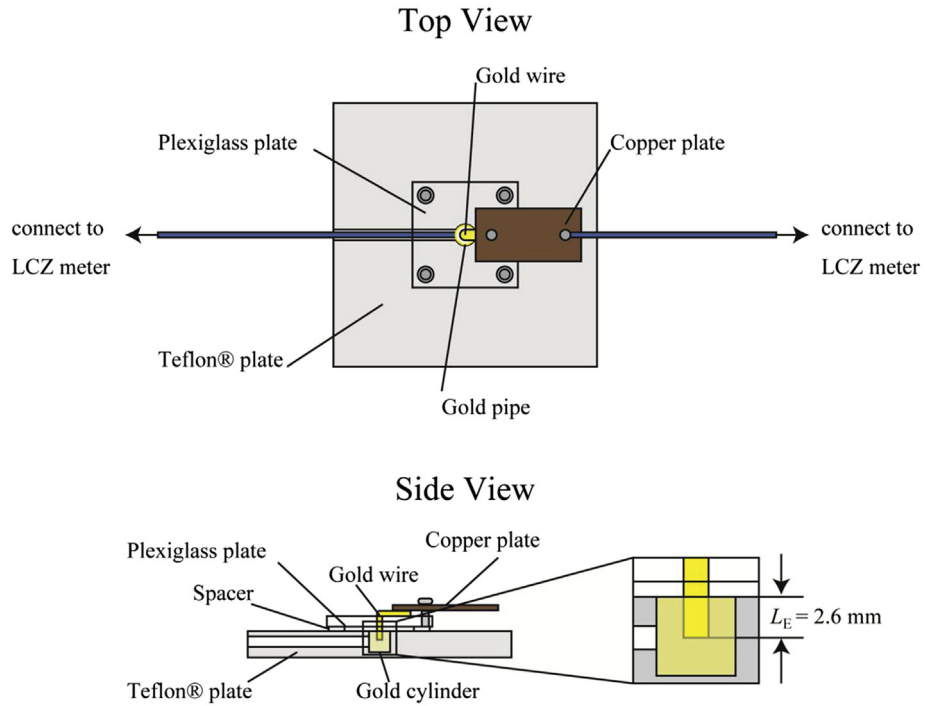
Top View

Side View

$L_E = 2.6$ mm

Fig. 1. Schematic illustration of the electrode chamber to measure the electrical impedance of epithelial lumen.

engineered epithelial lumens on the cellular architectures and the electrical impedance by using our system.

Materials and methods

Madin−Darby Canine Kidney (MDCK) cells were provided from RIKEN CELL BANK. DMEM (Nacalai tesque) supplemented with 10% fetal bovine replacement (Equitech-Bio) and 1% penicillin−streptomycin was used for culturing MDCK cells. Dulbecco's phosphate buffered saline (PBS(-)) was used for washing samples. Sodium chloride was dissolved with MilliQ water at various concentrations ranging from 2 mM to 1000 mM. Gold wires with the different diameters ranging from 50 μm−200 μm were purchased from Nilaco Co. Ltd., and they were used as a central
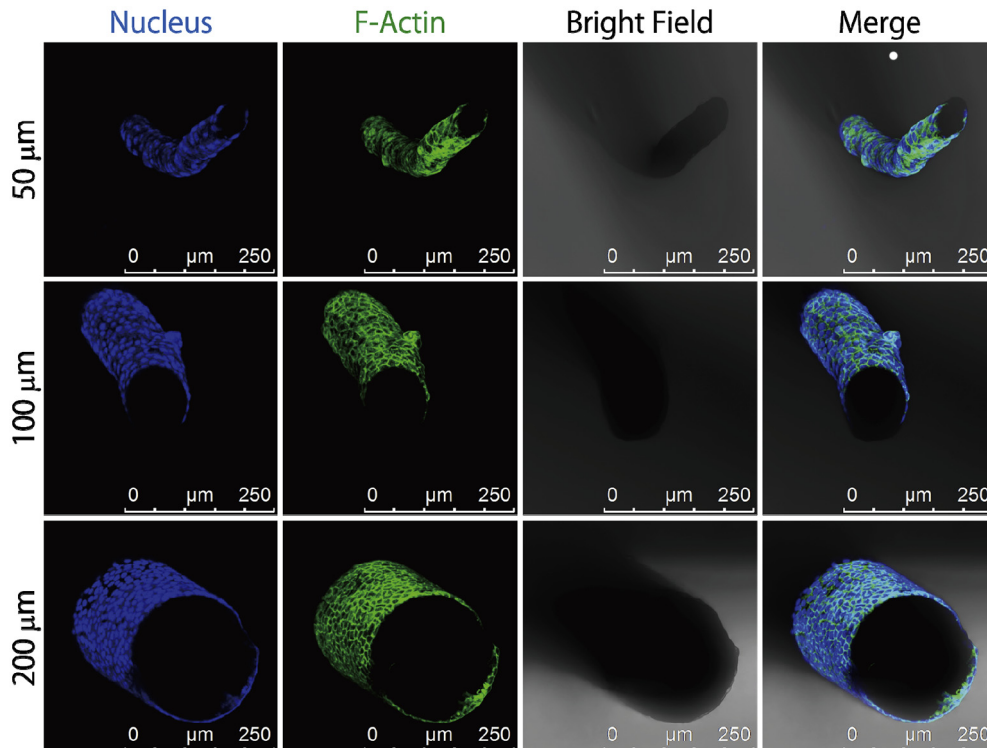

Fig. 2. Confocal laser scanning microscope images for the epithelial lumens constructed on the gold wires with various diameters.
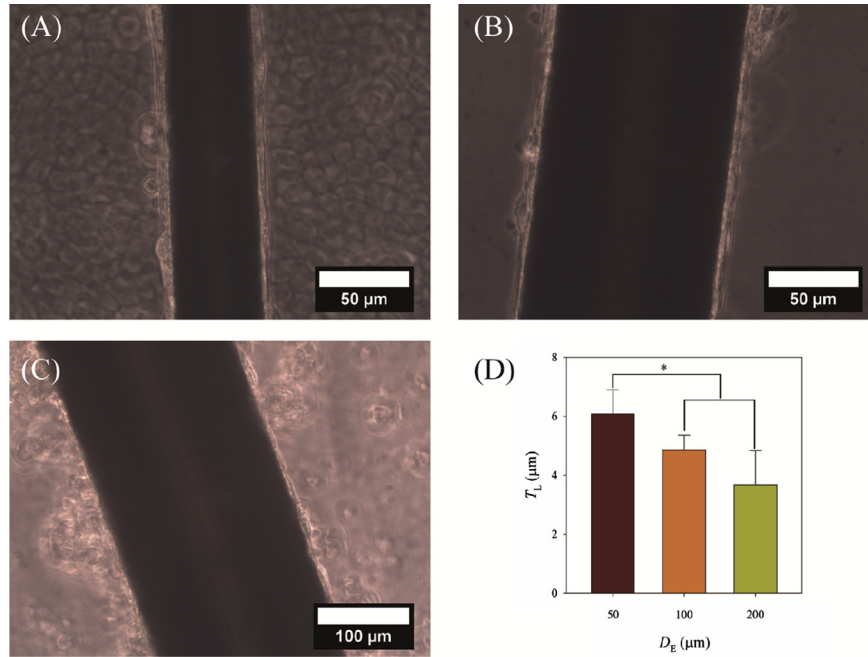
Fig. 3. Phase contrast optical microscope photographs for the epithelial lumens constructed on the gold wires with various diameters (D_E). The diameter of gold wires are (A): 50 μm, (B): 100 μm, and (C) 200 μm. (D): An effect of the diameter of gold wire on the thickness of epithelial lumen (T_L). An asterisk indicates a significance of $p < 0.05$.

electrode that is shown in Fig. 1. The gold pipe with the outer diameter of 4.0 mm and the inner diameter of 3.8 mm was purchased from Nilaco Co. Ltd, and it was used as an outer electrode that is shown in Fig. 1.

The epithelial lumens with various diameters were constructed by culturing MDCK cells on the surface of the gold wires. To facilitate attachment of MDCK cells onto the surface of the gold wires, the gold wires were coated with type I collagen (Cellmatrix® Nitta Gelatin Inc.). The gold wires were put into each wells of 6-well cell culture plate. MDCK cells were seeded onto the surface of gold wires at the cell density of 1.0×10^6 cells/mL. The medium was exchanged by every two days.

The samples cultured for 10 days were washed twice with PBS(-) and then they were fixed with 4 wt.% paraformaldehyde at 4 °C for 30 min. Next, the samples were washed four times with PBS(-) and they were immersed into 0.5 wt.% triton X100 at room temperature for 30 min. Then, the samples were washed twice with PBS(-) and they were immersed into 1.0% bovine serum albumin solution at room temperature for 6 h. Nuclei and F-actin of the samples were respectively labeled with Cytox® Blue (Molecular probes) that is diluted 1000-fold with PBS(-) and Alexa® 488 conjugated phalloidin (Molecular probes) that is diluted 150-fold with PBS(-) for overnight after washing the samples twice with PBS(-). Paxillin was labeled with the mouse monoclonal anti-paxillin antibody (BD Biosciences) that is diluted 100-fold with PBS(-) for overnight, and then the samples treated with the Alexa® 488 conjugated chicken monoclonal anti-mouse IgG antibody (Molecular probes) that is diluted 1000-fold with PBS(-) for 6 h. ZO-1 was labeled with the mouse monoclonal anti-ZO-1 antibody (Invitrogen) that is diluted 200-fold with PBS(-) for overnight, and then the samples treated with the Alexa® 488 conjugated chicken monoclonal anti-mouse IgG antibody (Molecular probes) that is diluted 1000-fold with PBS(-) for 6 h. The morphologies for the samples were observed by using a confocal laser scanning microscope (CLSM) (Leica TCS-SP5).

The schematic illustration for the system to measure the electrical impedance was shown in Fig. 1. An electrode chamber consists of a gold wire (central rod-like electrode) and a gold pipe (outer electrode). The outer surface of the gold pipe was completely shielded with the silicone gel (KE-104Gel, Shin-Etsu Chemical Co., Ltd.) and the mold made by PTFE. The electrode chamber was put into an aluminum cases to reduce noise. The electrode chamber was
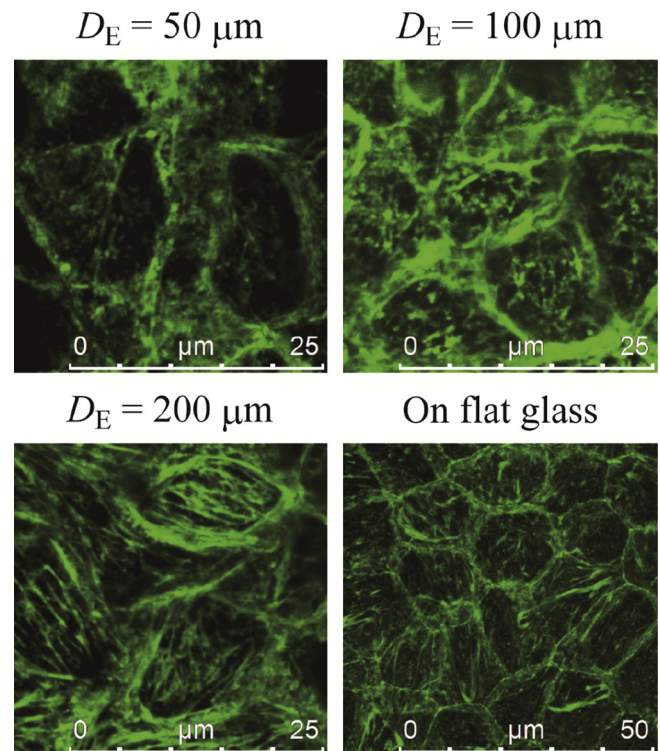

Fig. 4. F-actin expression patterns for the epithelial lumens constructed on the gold wires and the epithelial cell sheet constructed on the flat glass.

connected with the LCZ meter (2340 LCZ meter, NF Instruments Co., Ltd.) via coaxial cables and it was placed in an incubator at 37 °C.

The sodium chloride aqueous solutions and Leibovitz's L15 medium (Gibco) were filled into the gold pipe. The sample was placed at the center of the outer electrode by passing through a pore of plexiglass plate fixed on the PTFE mold. The electrical impedances $|Z|$ at the different frequency ranging from 10 Hz to 1.0 MHz were measured. To measure the electrical impedance, the alternating electric voltage with the amplitude of 60 mV was applied to the samples. According to the literature, the alternating electric voltage does not affect the electrical parameters of the epithelial cell sheets [10].

Results and discussion

Effects of the diameter of gold wire on morphologies of epithelial lumen

The confocal laser scanning microscope images for the samples are shown in Fig. 2. The surface of the gold wires was completely covered with the MDCK cell sheet, irrespective of the diameter of gold wire (D_E). Fig. 3 shows the phase contrast microscope photographs for the samples. The thicknesses of the MDCK cell sheets constructed on the gold wires with the diameters of 100 μm and 200 μm were thicker than that on the gold wire with the diameter of 50 μm. The result indicates that the diameter of the gold wire affects the morphology of the epithelial lumen. To investigate the effects of the diameter of gold wire on the cellular morphologies, we observed the expression patterns of F-actin, paxillin, and ZO-1 for the epithelial lumens constructed on the gold wire.

Fig. 4 shows the expression patterns of F-actin for the epithelial lumens constructed on the gold wires and the epithelial cell sheet constructed on the flat glass. At the $D_E = 200$ μm and on the flat glass, long actin stress fibers were observed in almost cells and they aligned parallel to a long axis of cell. Below $D_E = 100$ μm, mesh-like morphologies consisted of short actin stress fibers were observed, and the orientation of fiber was random. Silberzan et al. showed that the action stress fibers orient perpendicular to the long axis of glass wire below the diameter of 80 μm, whereas the orientation of actin fibers is not observed on the glass wire above the diameter of 80 μm [12]. However, although the epithelial lumen was constructed below the critical wire diameter (at $D_E = 50$ μm), there was no correlation between the orientation direction of F-actin fibers and the long axis of gold wire. No macroscopic orientation of F-actin fibers on our system might be attributed to the difference in the coating proteins, because the alignment of collagen fibrils affects the orientation of cells and actin stress fibers [13,14].

The curvature of gold wire increases with decreasing D_E. On the gold wire with the high curvature, a basal cell membrane of MDCK cells could be highly bended. Because the actin stress fibers are expressed along the basal cell membrane, formation of long actin stress fiber under the high curvature conditions requires to bend the fibers. However, the actin stress fibers have a long persistence length (~17.7 μm) [15], resulting in a large bending energy. Therefore, elongation of the actin stress fiber could be inhibited by the large bending energy under the high curvature conditions. We believe that the length of actin stress fibers determined by the bending strain of the basal cell membrane which increases with increasing the curvature of the gold wire.

To investigate the formation of focal adhesion (FA), we observed the expression pattern of paxillin, that is the protein localizes to the FA [16], for the epithelial lumens on the gold wires and the epithelial cell sheet on the flat glass. The expression patterns of paxillin are shown in Fig. 5A. On the gold wires with the diameter of 50 m and 100 μm, we found the scattered expression of spot-like FAs. By contrast, the expression patterns of FAs on the gold wire with the diameter of 200 μm and the flat glass were similar to the F-actin fiber. Because the paxillin localizes at the ends of actin stress fiber [16], the expression patterns of paxillin depend on the
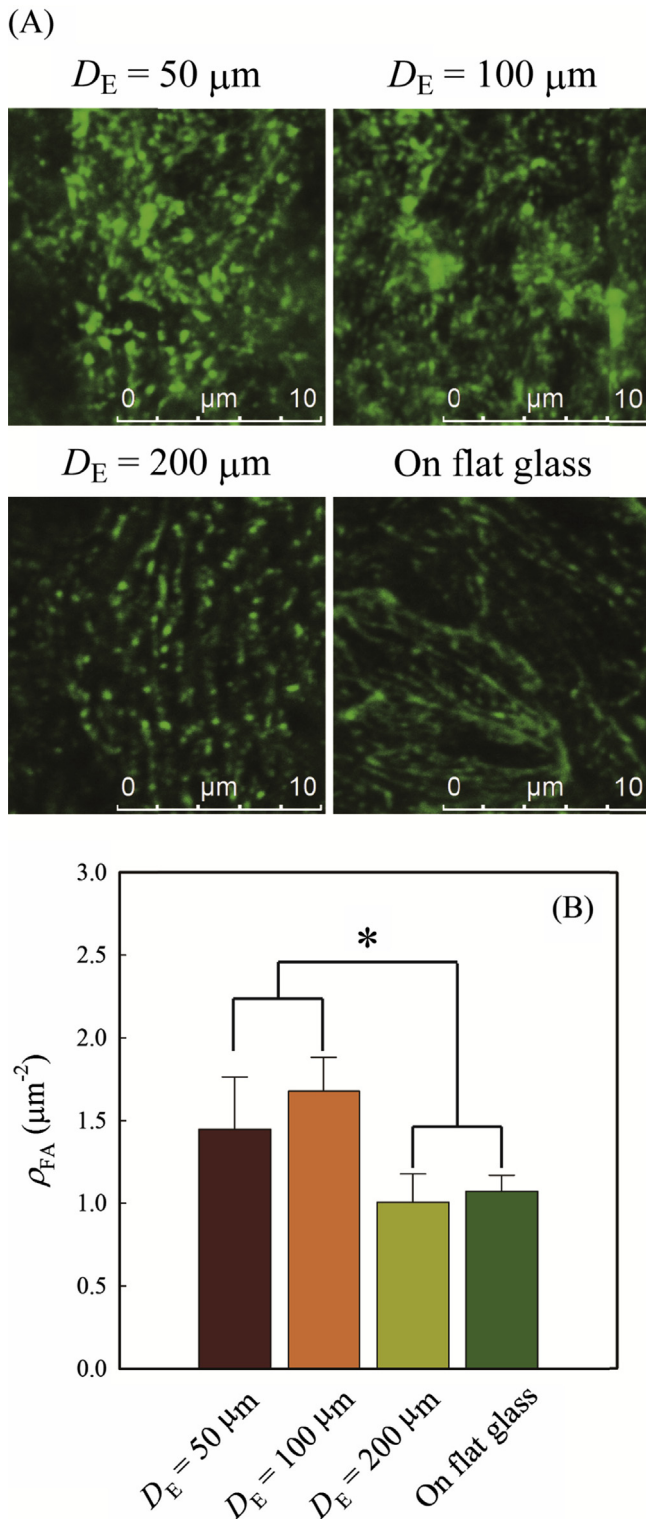

Fig. 5. (A): Expression patterns of paxillin for the epithelial lumens constructed on the gold wires and the epithelial cell sheet constructed on the flat glass. (B): Effect of diameter of gold wire on the focal adhesion density. The error bar indicates the standard deviation ($n = 3$). An asterisk indicates a significance of $p < 0.05$.
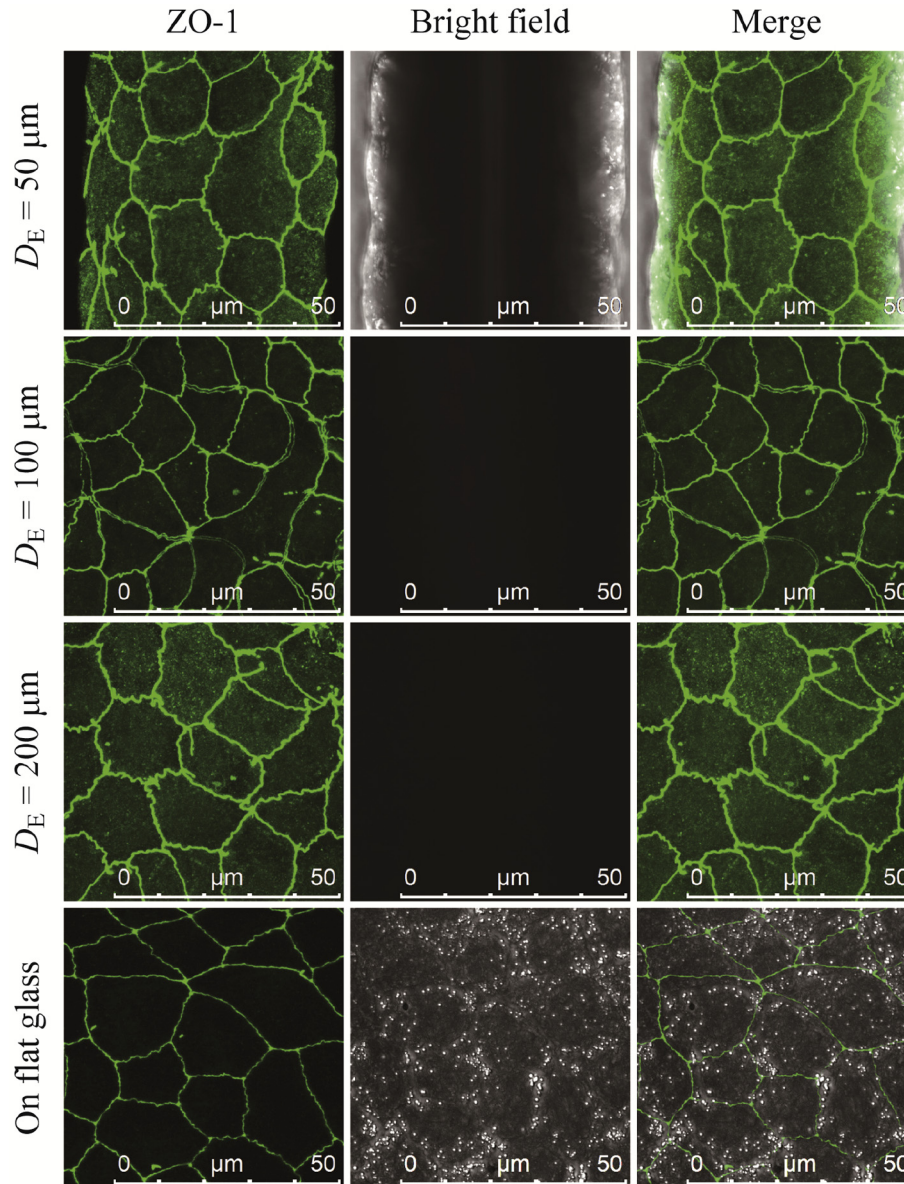
Fig. 6. Expression patterns of ZO-1 for the epithelial lumens constructed on the gold wires and the epithelial cell sheet constructed on the flat glass.

expression patterns of F-actin. The scattered expression patterns of spot-like FAs found at $D_E = 50$ μm and $D_E = 100$ μm are attributed to the mesh-like morphology consisted of many short actin fibers. By contrast, the long actin stress fibers aligned parallel to the long axis of cell result in the fiber-like expression pattern observed at $D_E = 200$ μm. To quantitatively characterize the difference in adhesion of cells onto the surface of gold wire, we measured the FA density which is defined as a number of FAs per unit area. The FA density for the epithelial lumens below $D_E = 100$ μm was significantly higher than those on the gold wire with the diameter of 200 μm and on the flat glass, as shown in Fig. 5B. The result was consistent with the previous reports [12]. The increase in FA density below $D_E = 100$ μm implies that the increase in adhesion force of MDCK cells onto the gold wire surface.

The barrier function of epithelial sheets is attributed to the tight junction (TJ) [17]. To characterize the formation of TJ of the epithelial lumens, we observed ZO-1 expression. ZO-1 is an intra-cellular protein and interacts with TJ-related proteins, such as claudins and occludin. Fig. 6 shows that ZO-1 was localized at an interface between adjacent MDCK cells, irrespective of D_E. Furthermore, the expression pattern of ZO-1 on the gold wires was similar to that on the flat glass. Many reports shows that MDCK cells cultured on the flat glass are tightly connected by TJ [18–20]. Therefore, the results indicate that MDCK cells on the gold wire construct the functional TJ.

Characterization of electrical impedance of epithelial lumens constructed on the gold wire

Conventional systems for measuring electrical impedance of epithelial cellular sheets have employed the sandwiched geometries in which the epithelial cell sheet was constructed on the water permeable membrane placed between two parallel electrodes [21]. By contrast, the system in which the epithelial cell sheet directly
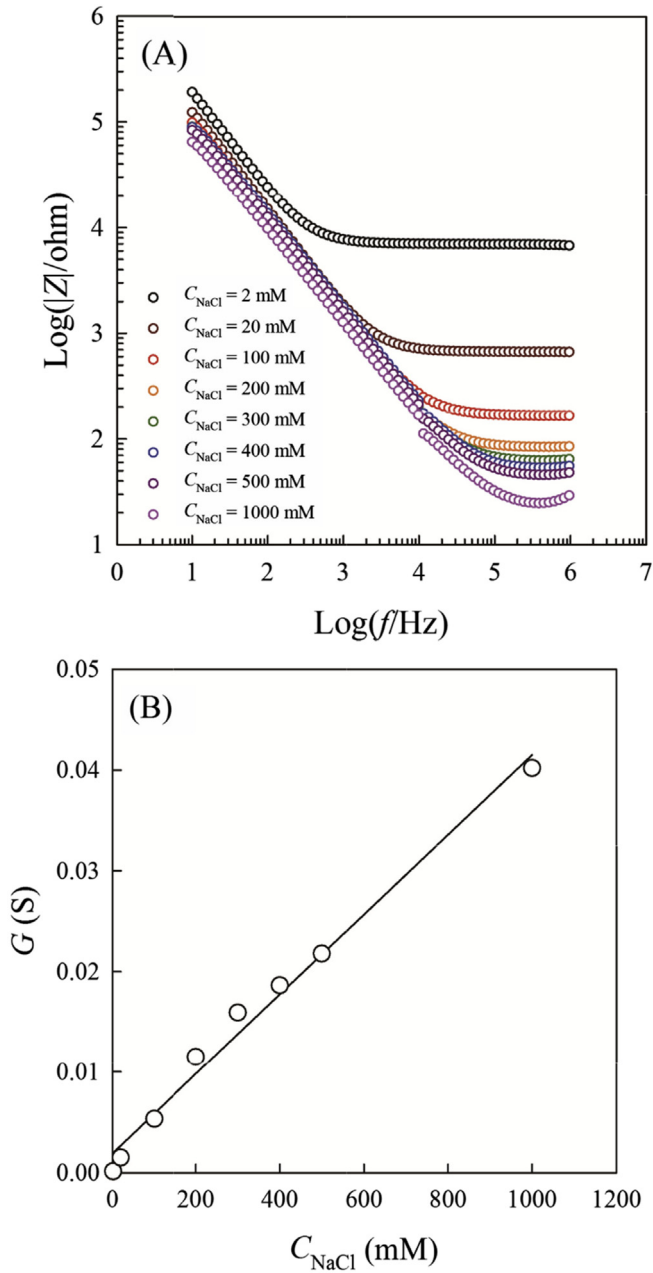
Fig. 7. (A): Electrical impedance spectra for the aqueous sodium chloride solutions with various concentrations. (B): Sodium chloride concentration dependence of the electrical conductance (G) at the plateau region which was observed in Fig. 7(A). The solid line was drawn by linear regression.

Fig. 8. (A)–(C): Electrical impedance spectra for the epithelial lumens constructed on the gold wires with various diameters. The error bar indicates the standard deviation (n = 3).

constructed on a surface of plate-like gold electrode has been reported [10]. Although there is a difference in electrode geometry, the results obtained from both systems approximately agreed [10]. Since our system corresponds to the latter one, the results obtained by using our system could be essentially same quality with the result obtained by using the conventional systems.

To test the utility for our electrical impedance measurement system, the electrical impedance spectra for aqueous sodium chloride solutions with various concentrations were measured. The electrical impedance spectra were shown in Fig. 7A. At the low frequency, the electrical impedance rapidly decreased with increasing the frequency. This rapid decrease could be attributable
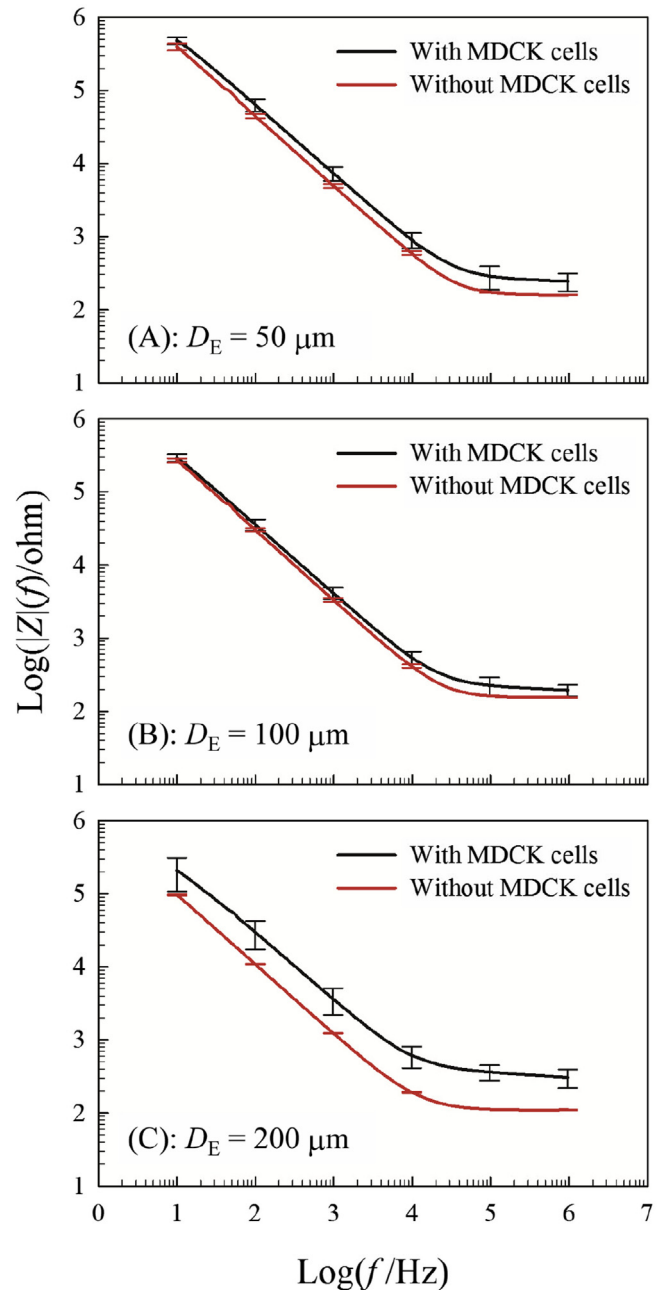
to the direct electrical conductivity. Furthermore, the electrical conductance (G), which can be calculated from the impedance and the phase spectra, at the plateau region linearly increased with increasing the sodium chloride concentration. The results could validate the reliability of our system, because the electrical conductivity of salt solution is generally proportional to the molarity [22].

The electrical impedance spectra ($|Z|(f)$) for the samples with and without MDCK cells were shown in Fig. 8A–C. In the experimental frequency range, $|Z|(f)$ for the samples with MDCK cells were higher than those for the samples without MDCK cells. Especially, the difference at $D_E = 200$ µm was larger than those
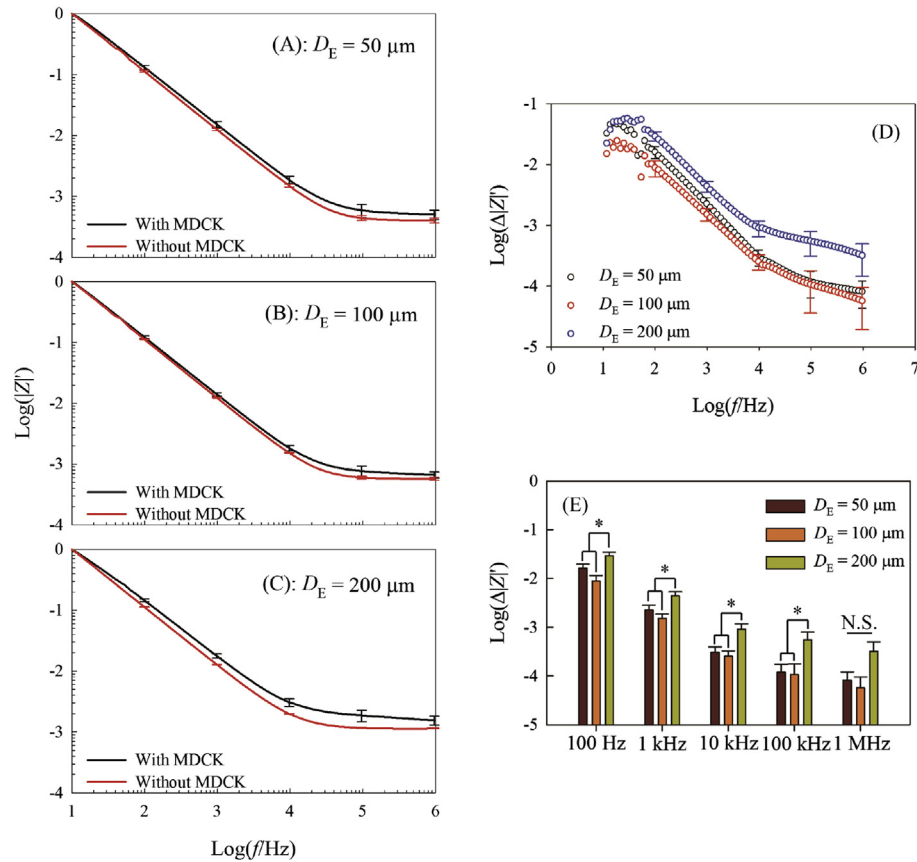
Fig. 9. (A)−(C): Normalized electrical impedance spectra for the epithelial lumens constructed on the gold wires with various diameters. (D): Differential electrical impedance spectra calculated by subtracting the normalized electrical impedance spectrum for the sample without MDCK cells from that with MDCK cells. (E): Comparison of the difference in the normalized electrical impedance at various frequencies. The error bar indicates the standard deviation ($n = 3$). An asterisk indicates a significance of $p < 0.05$. N.S. means not significant.

below $D_E = 100$ μm. The electrical impedance depends on the geometric factors of electrode chamber, such as the distance from the surface of inner electrode to the outer electrodes and the length of gold wire immersed into the L15 medium (L_E). Therefore, we cannot compare the electrical impedance spectra for the samples with different electrode diameters. In addition, although we made an effort to immerse the gold wire at the constant L_E ($= 2.6$ mm), it could be slightly different in each measurements. The difference in L_E affects the absolute value of electrical impedance. Therefore, we must correct the effects of the geometric factors on the electrical impedance spectra for comparing the electrical impedance spectra. The difference in the geometrical factors can be canceled by normalizing the electrical impedance by using the following equation:

$$|Z|'(f) = \frac{|Z|(f)}{|Z|_{10\,Hz}}$$

where the $|Z|_{10\,Hz}$ are the impedance value at 10 Hz. The normalized electrical impedance spectra were shown in Fig. 9A−C. The normalized electrical impedance spectra for the samples with the MDCK cells were also higher than that for the samples without the cells. The difference in $|Z|'(f)$ could be attributed to the barrier function of epithelial lumen on the gold wire. To investigate the effect of electrode diameter on the barrier function of the epithelial lumens, we compared the difference between $|Z|'(f)$ for the samples with and without MDCK cells ($\Delta|Z|'(f)$) (Fig. 9D−E). In the frequency

range from 100 Hz to 100 kHz, $\Delta|Z|'(f)$ at $D_E = 200$ μm was significantly higher than those below $D_E = 100$ μm. The result indicates that the barrier function of the epithelial lumen was disrupted by increasing the curvature of substrate. Although ZO-1 expression patterns for the epithelial lumens were not dependent on the gold wire diameter and indicate the formation of functional TJ, there was a significant difference in the barrier function. Since TJ is the protein complex consisted of various proteins, such as many types of claudins and occludin [17], the difference in curvature of gold wire probably alters the expression patterns of other TJ-related proteins. In addition, we showed the increase in curvature of gold wire modifies various cell architectures. Therefore, the disruption of barrier function is possibly attributed to the changes in cell architectures with decreasing the diameter of gold wire (or with increasing the curvature of gold wire).

Fig. 10 shows a phase contrast microscope photograph for the sample after measurement. The epithelial lumen was remained on the gold wire without damaged parts. The result showed that the electric impedance measurement of our system does not damage the sample.

Conclusion

The diameter of gold wire affects various cellular architectures. The cellular architecture for the epithelial lumen constructed on the gold wire with the diameter of 200 μm is similar to that for the MDCK cell sheet constructed on the flat glass. By contrast, the short
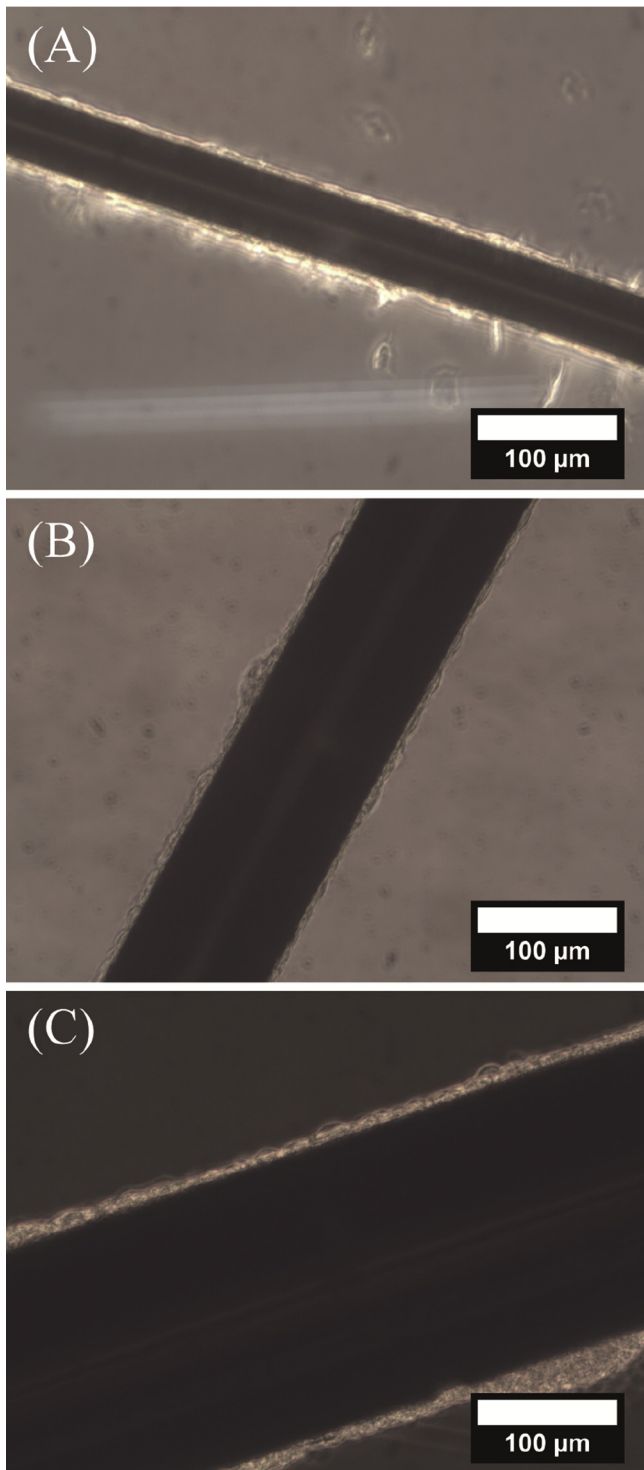
Fig. 10. Phase contrast optical microscope photographs for the samples after the electrical impedance measurement. The diameter of gold wires are (A): 50 μm, (B): 100 μm, and (C) 200 μm.

actin stress fibers and the high FA density were observed for the samples constructed below $D_E = 100$ μm. The changes in cellular architectures with decreasing D_E are possibly attributed to the increase in curvature of gold wire. To characterize the barrier function of epithelial lumens constructed on the gold wire, we developed the system to measure the electrical impedance spectra for the epithelial lumens with various diameters. The sodium chloride concentration dependence of electrical impedance spectra validated the reliability of our system. The electrical impedance for the epithelial lumen at $D_E = 200$ μm was significantly higher than those below $D_E = 100$ μm. The decrease in the electrical impedance under high curvature conditions might be attributable to the differences in cell architectures.

Acknowledgment

References

[1] Amasheh S, Meiri N, Gitter AH, Schöneberg T, Mankertz J, Schulzke JD, et al. Claudin-2 expression induces cation-selective channels in tight junctions of epithelial cells. J Cell Sci 2002;115:4969–76.

[2] Anderson JN, Itallie CMV. Tight junctions and the molecular basis for regulation of paracellular permeability. Am J Physiol Gastrointest Liver Physiol 1995;269:G467–75.

[3] Sekine H, Shimizu T, Sakaguchi K, Dobashi I, Wada M, Yamato M, et al. In vitro fabrication of functional three-dimensional tissues with perfusable blood vessels. Nat Comm 2013. http://dx.doi.org/10.1038/ncomms2406.

[4] Takebe T, Sekine K, Enomura M, Koike H, Kimura M, Ogaeri T, et al. Vascularized and functional human liver from an iPSC-derived organ bud transplant. Nature 2013;499:481–4.

[5] Sadr N, Zhu M, Osaki T, Kakegawa T, Yang Y, Moretti M, et al. SAM-based cell transfer to photopatterned hydrogels for microengineering vascular-like structures. Biomaterials 2011;32:7479–90.

[6] Furusawa K, Mizutani T, Machino H, Yahata S, Fukui A, Sasaki N. Application of multichannel collagen gels in construction of epithelial lumen-like engineered tissues. ACS Biomater Sci Eng 2015;1:539–48.

[7] Springer ML, Lp TK, Blau HM. Angiogenesis monitored by perfusion with a space-filling microbead suspension. Mol Ther 2000;1:82–7.

[8] Dvorak HF, Nagy JA, Dvorak JT, Dvorak AM. Identification and characterization of the blood vessels of solid tumors that are leaky to circulating macromolecules. Am J Pathol 1988;133:95–109.

[9] Powell DW. Barrier function of epithelia. Am J Physiol Gastrointest Liver Physiol 1981;241:G275–88.

[10] Wegener J, Sieber M, Galla H-J. Impedance analysis of epithelial and endothelial cell monolayers cultured on gold surfaces. J Biochem Biophys Methods 1996;32:151–70.

[11] Pappenheimer JR. Physiological regulation of transepithelial impedance in the intestinal mucosa of rats and hamsters. J Membr Biol 1987;100:137–48.

[12] Yevick HG, Duclos G, Bonnet I, Silberzan P. Architecture and migration of an epithelium on a cylindrical wire. Proc Natl Acad Sci U. S. A 2015;112:5944–9.

[13] Guido S, Tranquillo RT. A methodology for the systematic and quantitative study of cell contact guidance in oriented collagen gels. Correlation of fibroblast orientation and gel birefringence. J Cell Sci 1993;105:317–31.

[14] Huang NF, Okogbaa J, Lee JC, Jha A, Zaitseva TS, Paukshto MV, et al. The modulation of endothelial cell morphology, function, and survival using anisotropic nanofibrillar collagen scaffolds. Biomaterials 2013;34:4038–47.

[15] Gittes F, Mickey B, Nettleton J, Howard J. Flexural rigidity of microtubules and actin filaments measured from thermal fluctuations in shape. J Cell Biol 1993;120:923–34.

[16] Turner CE, Glenney Jr JR, Burridge K. Paxillin: a new vinculin-binding protein present in focal adhesions. J Cell Biol 1990;111:1059–68.

[17] Alberts B, Johnson A, Lewis J, Morgan D, Raff M, Roberts K, et al. Molecular biology of the cell 6th edition. Garland Science; 2015.

[18] Inai T, Kobayashi J, Shibata Y. Claudin-1 contributes to the epithelial barrier function in MDCK cells. Euro J Cell Biol 1999;78:849–55.

[19] Gonzalez-Mariscal L, Chávez de Ramírez B, Cereijido M. Tight junction formation in cultured epithelial cells (MDCK). J Membr Biol 1985;86:113–25.

[20] Stevenson BR, Siliciano JD, Mooseker MS, Goodenough DA. Identification of ZO-1: a high molecular weight polypeptide associated with tight junction (Zonula Occludens) in a variety of epithelia. J Cell Biol 1986;103:755–66.

[21] Erben M, Decker S, Franke H, Galla H-J. Electrical resistance measurements on cerebral capillary endothelial cells — a new technique to study small surface areas. J Biochem Biophys Methods 1995;30:227–38.

[22] Atkins PW. Physical chemistry 6th edition. Oxford University Press; 1988.